



Predicting Magnetic Remanence of NdFeB Magnets from Composition

Yun Zhang¹ · Xiaojie Xu¹

Received: 22 April 2021 / Accepted: 27 April 2021 / Published online: 2 September 2021
© The Author(s), under exclusive licence to Springer Science+Business Media, LLC, part of Springer Nature 2021

Abstract

The composition of NdFeB-type magnets has a great impact on their performance. To enhance the remanence of the magnet, Zr and Co are alloyed into the starting materials. To develop an empirical equation that calculates the remanence based on alloying elements, the multiple linear regression model is developed in this work. It elucidates the statistical relationship between alloying elements content and magnetic remanence for Zr/Co-alloyed NdFeB magnets. The model is simple and straightforward and has a high degree of accuracy and stability, which contributes to fast low low-cost magnetic remanence estimations.

Keywords Permanent magnet · Remanence · Composition · NdFeB · Multiple linear regression

NdFeB-type magnets are widely used in applications, including consumer electronics, acoustics, magnetic resonance images, computer peripherals, and office automation [1]. For example, automotive control systems, servo and linear drives, and high torque motors are among the major markets [2–6]. Besides, NdFeB magnets are used in high-temperature superconducting (HTS) maglev systems as magnetic rail construction [7–12]. Recently, superconducting MgB₂ discs are combined in a pair-type sandwich-like arrangement with a permanent NdFeB magnet to provide a trapped field [13–15].

In order to enhance the thermal stability, alloying elements are added to the composition to increase the Curie temperature, decrease the temperature coefficient of residual magnetization (B_r), and increase the coercivity (H_c). Heavy rare-earth (HRE) elements, such as Dy and Tb, are common choices, which, however, decrease the saturation magnetization and thus reduce the remanence and energy products $(BH)_{max}$. Moreover, HREs are limited natural resources, which result in a substantial increase in cost. Thus, HRE-free NdFeB magnets with other types of alloying elements have been researched extensively. Most NdFeB-type magnets are manufactured by starting with melt-quenching

nanocrystalline materials. The nanocrystalline materials are then bonded and hot deformed into components, and undergo sintering processes to form highly dense products [16]. The composition, microstructure, and processing of NdFeB-type magnets are critical factors in production of high-performance permanent magnet components [16–18]. Especially, the type and amount of additives significantly determine magnetic performance. To achieve high $(BH)_{max}$, the remanence must be high, which requires a minimal fraction of the minor non-ferromagnetic phases. For instance, refractory elements, such as Zr, are found to enhance the coercivity by suppressing the formation of α -Fe, inhibiting grain coarsening and also forming borides at the grain boundaries. However, the addition of Zr leads to the reduction in remanence due to the formation of a nonmagnetic boride phase [19–21]. On the other hand, the addition of Co increases the Curie temperature without decreasing the remanence [1]. Experimental approaches have been carried out to modify the composition of Zr/Co-alloyed NdFeB magnets and assess the effects of additives on the magnetization, thermal stability, and corrosion resistance [22]. But these approaches are resource-intensive and time-consuming as there may be many combinations of possible alloying elements. Furthermore, the effects of constituting elements on the remanence are complex. Therefore, it is of great importance to develop a method to estimate the remanence of the doped magnet through composition.

Empirical equations have been used to calculate important physical parameters of alloys based on composition.

✉ Yun Zhang
yzhang43@ncsu.edu
Xiaojie Xu
xxu6@ncsu.edu

¹ North Carolina State University, Raleigh, NC 27695, USA

Recently, data-driven methods are developed for materials design and discoveries, in contrast to traditional synthesize-test-repeat approaches [23–25]. For example, many methodologies have been applied to estimate and calculate martensite start temperature based on steel composition [26–28]. But there is very limited research on estimating remanence of NdFeB-type magnets through the content of alloying elements [29]. In this study, we develop the multiple linear regression (MLR) model with interactions based on the QR (Q stands for an orthogonal matrix and R for an upper triangular matrix) decomposition algorithm [30–34] to elucidate the statistical relationship between alloying elements content and magnetic remanence for NdFeB magnets. The model is simple, straightforward, and accurate that contributes to fast low-cost estimations of magnetic remanence and understandings of which are based on alloying elements content. It could serve as a guideline for designing the composition of Zr/Co-alloyed NdFeB magnets with optimal remanence.

The data in Table 1 (columns 2–7) are from [35]. Alloying elements (Nd, Co, Zr, B, and Fe) content is used as the descriptor. Performance of the proposed MLR models is assessed with the *CC* (correlation coefficient) and *RMSE* (root mean square error).

The MLR model for $Br(T)$ is: $Br^{MLR} = -0.38674Nd + 0.048379Co - 0.309Zr + 5.6362B - 0.0040387Fe + 0.0048496Nd \times Co + 0.0010112Nd \times Zr - 0.078295Nd \times B + 0.007142Nd \times Fe + 0.00066895Co \times Zr - 0.07456Co \times B + 0.00094539Co \times Fe - 0.097038Zr \times B + 0.0074643Zr \times Fe - 0.060152B \times Fe$, which shows good alignment between predictions and experimental values, as visualized in Figure 1 (legend “MLR Prediction”). The *CC* and *RMSE* for T_c are 98.34% and 0.0044, respectively, representing good performance.

Performance of our final MLR model is compared with that based on the SVR (support vector regression) [36], which has the *CC* and *RMSE* of 91.59% and 0.0101, respectively. Therefore, the MLR leads to improved performance.

Table 1 Data and different predictions

Index	Nd	Co	Zr	B	Fe	<i>Br(T)</i>		
						Experimental	SVR	MLR
1	10.5	4	0.0	6.2	79.3	0.690	0.690	0.687
2	9.0	1	2.0	6.0	82.0	0.631	0.633	0.637
3	11.0	3	3.0	6.0	77.0	0.612	0.613	0.615
4	9.5	4	3.0	5.8	77.7	0.655	0.650	0.655
5	10.0	0	2.5	6.0	81.5	0.652	0.649	0.647
6	9.5	0	1.5	6.2	82.8	0.640	0.640	0.638
7	11.5	4	1.5	6.6	76.4	0.632	0.634	0.634
8	11.0	0	1.0	6.4	81.6	0.662	0.662	0.663
9	10.5	2	1.5	5.8	80.2	0.656	0.656	0.664
10	11.0	5	2.0	5.6	76.4	0.693	0.651	0.690
11	10.0	3	2.0	6.4	78.6	0.660	0.654	0.650
12	9.0	5	2.5	6.4	77.1	0.627	0.626	0.627
13	9.0	3	1.0	5.6	81.4	0.644	0.644	0.640
14	9.5	2	0.0	6.6	81.9	0.685	0.685	0.687
15	10.5	1	3.0	6.6	78.9	0.617	0.615	0.621
16	10.0	5	1.0	6.0	78.0	0.671	0.671	0.677
17	11.5	1	0.0	5.8	81.7	0.646	0.646	0.646
18	11.5	2	2.5	6.2	77.8	0.617	0.617	0.614
Minimum	9.0	0	0.0	5.6	76.4	0.612	0.613	0.614
Mean	10.3	2.5	1.7	6.1	79.5	0.649	0.646	0.649
Median	10.3	2.5	1.8	6.1	79.1	0.649	0.648	0.646
Std	0.9	1.8	1.0	0.3	2.2	0.025	0.022	0.024
Maximum	11.5	5.0	3.0	6.6	82.8	0.693	0.690	0.690
CC w. Experimental <i>Br(T)</i>	-6.36%	26.52%	-59.60%	-18.43%	11.70%	-	91.59%	98.34%

Columns 2–6 contain alloying elements (Nd, Co, Zr, B, and Fe) content. Column 7 contains the target variable, experimental magnetic remanence $Br(T)$. Column 8 contains the predicted $Br(T)$ based on the SVR (support vector regression) from [36]. Column 9 contains the predicted $Br(T)$ based on the MLR (multiple linear regression) from the current study

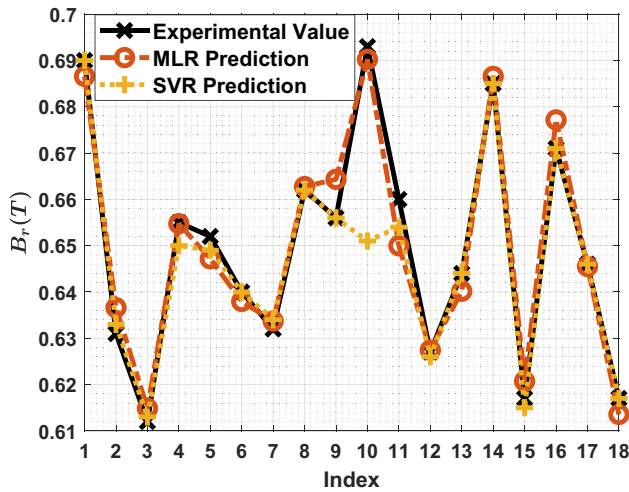


Fig. 1 The experimental vs. predicted $Br(T)$. The final MLR model, corresponding to the figure legend “MLR Prediction,” is from the current study. The figure legend “SVR Prediction” is obtained from [36] that is based on the support vector regression, whose numerical predictions are listed in Table 1

In addition, the MLR is simpler and more straightforward from the perspective of computations and implementations than the SVR.

Each term in the MLR model reflects the individual and combined effects of concentrations of alloying elements. Previous experimental results suggest that increasing amounts of Nd, Zr, and Fe generally lead to a decrease in Br, while increasing amounts of Co and B may lead to an increase in Br [36]. These effects of individual elements on Br have been captured by the MLR model, which are reflected by the positive and negative signs of relative terms qualitatively. The contribution of each term to Br is quantified by the corresponding coefficient. Furthermore, multi-element effects on changes in Br are also quantified by the MLR model. This revelation is more important in analyzing the synergistic effect of dopants on Br values than conventional single-element analysis since, practically, any change in the concentration of one element results in changes of

other elements. Therefore, the sign and absolute value of the coefficient of each dual-element term in the MLR model show the complex correlations within variations in concentrations of multiple elements. As presented by the model, the numerical relationship between Br and elemental compositions is no longer intuitive, which cannot be quantified by traditional assumptions through experimental approaches. For example, there are terms associated with the Fe concentration that show both positive and negative impacts on Br, which is seemingly contrary to the superficial assumption that an increase in the Fe concentration should result in a decrease in Br. However, by adjusting the Fe concentration, concentrations of other elements vary as well, which may have either positive or negative impacts on Br to varying degrees. Thus, a comprehensive MLR model that captures the multi-element effects on Br with robust model performance is significantly useful to the alloying design of NdFeB permanent magnets.

Besides, the experimental data in the current study focus on doped-NdFeB samples that were processed through argon arc-melt and quenched as thin ribbon samples [35]. The sintering temperature for all the samples was between 670 °C and 720 °C, which minimizes the effects of the sintering temperature on the diffusion behavior at grain boundaries. It has been pointed out by previous research that the sintering behavior of NdFeB, particularly $Nd_{16}Fe_{76}B_8$, changes significantly between 800 °C and 900 °C due to the densification [37]. Beyond 900 °C, the densification and connectivity between grains largely increase. For future work on predictions of Br or other magnetic properties through numerical methods, the inclusion of the sintering temperature might be needed if the samples are processed differently and/or influenced greatly by the temperature.

To give an example of an extended model of adding an additional descriptor, we build the model, Br^{MLR_2} , based on the old one, Br^{MLR} , with the additional descriptor of the volume content of excess α -Fe, denoted as $eaFe$. The model, Br^{MLR_2} , is expressed as $Br^{MLR_2} = Br^{MLR} + 0.010045 eaFe \times Nd - 0.0014618 eaFe \times Fe - 4.1945 \times 10^{-6} eaFe^2 \times Nd \times Fe - 6.9725 \times 10^{-7} eaFe^2 \times Co \times Fe + 1.2243 \times 10^{-5}$

Table 2 Data used to build Br^{MLR_2} and performance of Br^{MLR_2}

Nd	Co	Zr	B	Fe	eaFe	Br(T)		Reference
						Experimental	MLR_2	
12.6	11.6	0.5	6.0	69.3	40.0	1.130	1.139	[38]
12.6	11.6	0.5	6.0	69.3	50.0	1.110	1.107	[38]
12.6	0.0	0.0	6.0	81.4	37.5	0.630	0.630	[39]
12.6	11.6	0.0	6.0	69.8	37.5	0.550	0.550	[39]
12.6	11.6	0.5	6.0	69.3	10.0	0.860	0.855	[40]
12.6	11.6	0.5	6.0	69.3	37.5	1.140	1.137	[40]
16.0	11.6	0.5	6.0	65.9	10.0	0.920	0.920	[40]
16.0	11.6	0.5	6.0	65.9	37.5	1.070	1.070	[40]

$eaFe^2 \times Zr \times Fe + 8.3754 \times 10^{-6} eaFe^2 \times B \times Fe$. The data used to build Br^{MLR_2} are listed in Table 2. It can be seen that Br^{MLR_2} leads to rather accurate predictions. The model, Br^{MLR_2} , still works for magnets without excess α -Fe, including the data in Table 1 and one out-of-sample data point with Nd=12.6, Co=11.6, Zr=0.5, B=6.0, and Fe=69.3 [38]. It shows that the statistical relationship among initial composition is still valid and generalized. The additional terms in the formula are expressed involving only the added descriptor, the volume content of excess α -Fe. From the equation of Br^{MLR_2} , dominated terms are correlations among excess α -Fe, Nd, and Fe, which follow the same qualitative impact on Br. Previous research on NdFeB/ α -Fe nanocomposite magnets indicate that the excess α -Fe plays a role in tailoring the microstructure, such as the grain size, crystallographic perfection, phase assemblage, and grain alignments [38–40], and thus affects the magnetic performance. For future work, other descriptors can be included for model development. Processing parameters, including temperature, sintering time, and hot-press pressure, can be added if a series of experiments are conducted. We develop the multiple linear regression (MLR) model to predict magnetic remanence based on alloying elements content for NdFeB magnets. The initial model uses elemental contents of Nd, Co, Zr, B, and Fe as descriptors, and the extended model adds one more descriptor, the volume content of excess α -Fe. The models are simple, straightforward, and highly accurate, suggesting their usefulness to quantify the relationship between alloying elements content and magnetic remanence. Nonetheless, microstructural textures have significant effects on remanence values and are affected not only by the composition but processing parameters, such as temperature, sintering time, and hot-press pressure. However, parameters to describe microstructural textures are difficult to define and obtain. For example, the grain size, grain alignment, composition of secondary phases, interfaces at the triple junction, and density are typical characteristics used to correlate with magnetic properties. Unless a systematic definition method is adopted, microstructural comparisons between samples are highly subjective and incomplete. These factors limit the capability to incorporate microstructural parameters into our models. In most studies, qualitative or semi-quantitative correlations were found, but a mathematical description was barely achieved. Should a systematic and quantitative set of microstructural parameters be established, further model development may help reveal a quantitative relationship between microstructural parameters and magnetic remanence.

Data Availability Statement The data that support the findings of this study are available within the article.

References

- Kim, A.S., Camp, F.E.: High performance NdFeB magnets. *J. Appl. Phys.* **79**(8), 5035–5039 (1996). <https://doi.org/10.1063/1.361566>
- Li, M., Wang, Z., Wang, Y., Li, J., Viehland, D.: Giant magnetoelectric effect in self-biased laminates under zero magnetic field. *Appl. Phys. Lett.* **102**(8), 082404 (2013). <https://doi.org/10.1063/1.4794056>
- Li, M., Dong, C., Zhou, H., Wang, Z., Wang, X., Liang, X., Lin, Y., Sun, N.X.: Highly sensitive DC magnetic field sensor based on nonlinear ME effect. *IEEE Sens. Lett.* **1**(6), 1–4 (2017). <https://doi.org/10.1109/LSENS.2017.2752216>
- Wang, Y., Hasanyan, D., Li, M., Gao, J., Li, J., Viehland, D.: Equivalent magnetic noise in multi-push-pull configuration magnetoelectric composites: Model and experiment. *IEEE Trans. Ultrason. Ferroelec. Freq. Cont.* **60**(6), 1227–1233 (2013). <https://doi.org/10.1109/TUFFC.2013.2686>
- Wang, Y., Hasanyan, D., Li, M., Gao, J., Viswan, R., Li, J., Viehland, D.: Magnetic field dependence of the effective permittivity in multiferroic composites, *physica status solidi (a)*, **209**(10), 2059–2062 (2012). <https://doi.org/10.1002/pssa.201228278>
- Li, M., Berry, D., Das, J., Gray, D., Li, J., Viehland, D.: Enhanced sensitivity and reduced noise floor in magnetoelectric laminate sensors by an improved lamination process. *J. Am. Cer. Soc.* **94**(11), 3738–3741 (2011). <https://doi.org/10.1111/j.1551-2916.2011.04659.x>
- Zhang, Y., Johnson, S., Naderi, G., Chaubal, M., Hunt, A., Schwartz, J.: High critical current density $Bi_2Sr_2CaCu_2O_x/Ag$ wire containing oxide precursor synthesized from nano-oxides. *Supercond. Sci. Tech.* **29**(9), 095012 (2016). <https://doi.org/10.1088/0953-2048/29/9/095012>
- Zhang, Y., Koch, C.C., Schwartz, J.: Formation of $Bi_2Sr_2CaCu_2O_x/Ag$ multifilamentary metallic precursor powder-in-tube wires. *Supercond. Sci. Tech.* **29**(12), 125005 (2016). <https://doi.org/10.1088/0953-2048/29/12/125005>
- Zhang, Y., Koch, C.C., Schwartz, J.: Synthesis of $Bi_2Sr_2CaCu_2O_x$ superconductors via direct oxidation of metallic precursors. *Supercond. Sci. Tech.* **27**(5), 055016 (2014). <https://doi.org/10.1088/0953-2048/27/5/055016>
- Sun, R., Zheng, J., Zheng, B., Qian, N., Li, J., Deng, Z.: New magnetic rails with double-layer Halbach structure by employing NdFeB and ferrite magnets for HTS maglev. *J. Magnet. Magn. Mat.* **445**, 44–48 (2018). <https://doi.org/10.1016/j.jmmm.2017.08.082>
- Song, H., Hunte, F., Schwartz, J.: On the role of pre-existing defects and magnetic flux avalanches in the degradation of $YBa_2Cu_3O_{7-x}$ coated conductors by quenching. *Acta Materialia* **60**(20), 6991–7000 (2012). <https://doi.org/10.1016/j.actamat.2012.09.003>
- Thieme, C.L.H., Gagnon, K.J., Coulter, J.Y., Song, H., Schwartz, J.: Stability of second generation HTS pancake coils at 4.2 K for high heat flux applications, *IEEE Trans. Appl. Supercond.* **19**(3), 1626–1632 (2009). <https://doi.org/10.1109/TASC.2009.2017914>
- Jiang, J., Bradford, G., Hossain, S.I., Brown, M.D., Cooper, J., Miller, E., Huang, Y., Miao, H., Parrell, J.A., White, M., Hunt, A., Sengupta, S., Revur, R., Shen, T., Kametani, F., Trociewitz, U.P., Hellstrom, E.E., Larbalestier, D.C.: High-performance Bi-2212 round wires made with recent powders. *IEEE Trans. Appl. Supercond.* **29**(5), 1–5 (2019). <https://doi.org/10.1109/TASC.2019.2895197>
- Shen, T., Bosque, E., Davis, D., Jiang, J., White, M., Zhang, K., Higley, H., Turqueti, M., Huang, Y., Miao, H., Trociewitz, U.: Stable, predictable and training-free operation of superconducting Bi-2212 Rutherford cable racetrack coils at the wire current density of 1000 A/mm². *Sci. Rep.* **9**(1), 1–9 (2019). <https://doi.org/10.1038/s41598-019-46629-3>

15. Aldica, G., Burdusel, M., Badica, P.: Trapped magnetic field in a (NdFeB)-(MgB₂) pair-type bulk magnet. *Physica C: Supercond. Appl.* **505**, 18–23 (2014). <https://doi.org/10.1016/j.physc.2014.07.001>
16. Brown, D., Ma, B.M., Chen, Z.: Developments in the processing and properties of NdFeB-type permanent magnets. *J. Magnet. Magn. Mat.* **248**(3), 432–440 (2002). [https://doi.org/10.1016/S0304-8853\(02\)00334-7](https://doi.org/10.1016/S0304-8853(02)00334-7)
17. Fan, M., Liu, Y., Jha, R., Dulikravich, G.S., Schwartz, J., Koch, C.C.: On the evolution of Cu-Ni-rich bridges of Alnico alloys with tempering. *J. Magnet. Magn. Mat.* **420**, 296–302 (2016). <https://doi.org/10.1016/j.jmmm.2016.07.040>
18. Fan, M., Liu, Y., Jha, R., Dulikravich, G.S., Schwartz, J., Koch, C.C.: On the formation and evolution of Cu-Ni-rich bridges of alnico alloys with thermomagnetic treatment. *IEEE Trans. Magn.* **52**(8), 1–10 (2016). <https://doi.org/10.1109/TMAG.2016.2555956>
19. Hirose, S., Tomizawa, H., Mino, S., Hamamura, A.: High-coercivity Nd-Fe-B-type permanent magnets with less dysprosium. *IEEE Trans. Magn.* **26**(5), 1960–1962 (1990). <https://doi.org/10.1109/20.104582>
20. Sagawa, M., Tenaud, P., Vial, F., Hiraga, K.: High coercivity Nd-Fe-B sintered magnet containing vanadium with new microstructure. *IEEE Trans. Magn.* **26**(5), 1957–1959 (1990). <https://doi.org/10.1109/20.104581>
21. Kim, A.S., Camp, F.E.: A high performance Nd-Fe-B magnet with improved corrosion resistance. *IEEE Trans. Magn.* **28**(5), 2151–2153 (1992). <https://doi.org/10.1109/20.179426>
22. Camp, F.E., Kim, A.S.: Effect of microstructure on the corrosion behavior of NdFeB and NdFeCoAlB magnets. *J. Appl. Phys.* **70**(10), 6348–6350 (1991). <https://doi.org/10.1063/1.349938>
23. Zhang, Y., Xu, X.: Yttrium barium copper oxide superconducting transition temperature modeling through Gaussian process regression. *Comput. Mat. Sci.* **179**, 109583 (2020). <https://doi.org/10.1016/j.commatsci.2020.109583>
24. Zhang, Y., Xu, X.: Predicting doped MgB₂ superconductor critical temperature from lattice parameters using Gaussian process regression. *Physica C: Supercond. Appl.* **573**, 1353633 (2020). <https://doi.org/10.1016/j.physc.2020.1353633>
25. Zhang, Y., Xu, X.: Curie temperature modeling of magnetocaloric lanthanum manganites using Gaussian process regression. *J. Magnet. Magn. Mat.* **512**, 166998 (2020). <https://doi.org/10.1016/j.jmmm.2020.166998>
26. Capdevila, C., Caballero, F., Garcia, C.: *Metal. Prog.* **46**, 108, ISIJ International. **42**(8), 894–902 (1944)
27. Kung, C.Y., Rayment, J.J.: Hardenability concepts with applications to steel. TMS-AIME, Warrendale, PA. 229–248 (1978)
28. Andrews, K.W.: Empirical formulae for the calculation of some transformation temperatures, *Journal of the Iron and Steel Institute*. pp. 721–727 (1965)
29. Jha R, Dulikravich, G.S., Colaço, M.J., Fan, M., Schwartz, J., Koch, C.C.: *Magnetic alloys design using multi-objective optimization, Properties and Characterization of Modern Materials*. pp. 261–284, (2017) Springer, Singapore. https://doi.org/10.1007/978-981-10-1602-8_22
30. Gentle, J.E.: *Numerical linear algebra for applications in statistics*. Springer Science & Business Media (2012)
31. Householder, A.S.: *The numerical treatment of a single nonlinear equation*. McGraw-Hill, New York (1970)
32. Nash, J.C.: *Compact numerical methods for computers: linear algebra and function minimisation*, CRC Press. (1990)
33. Vetterling, W.T., W.H.: *Press, Numerical recipes in Fortran: the art of scientific computing*, Cambridge University Press. (1992)
34. Stewart, G.W.: A parallel implementation of the QR-algorithm. *Parall. Comp.* **5**(1–2), 187–196 (1987). [https://doi.org/10.1016/0167-8191\(87\)90017-2](https://doi.org/10.1016/0167-8191(87)90017-2)
35. Lian, L.X., Liu, Y., Song, D.Y., Gao, S.J., Tu, M.J.: Study for effect of alloying element on magnetic properties of NdFeB magnets by artificial neural network. *J. Func. Mat.* **36**(8), 1178 (2005)
36. Cheng, W.: Prediction of magnetic remanence of NdFeB magnets by using novel machine learning intelligence approach—Support vector regression, 2014 IEEE 13th International Conference on Cognitive Informatics and Cognitive Computing. pp. 431–435 (2014). <https://doi.org/10.1109/ICCI-CC.2014.6921494>
37. Davies, B.E., Mottram, R.S., Harris, I.R.: Recent developments in the sintering of NdFeB. *Mat. Chem. Phys.* **67**(1–3), 272–281 (2001). [https://doi.org/10.1016/S0254-0584\(00\)00450-8](https://doi.org/10.1016/S0254-0584(00)00450-8)
38. Jurczyk, M., Gwan, P.B.: Magnets produced by hot pressing Nd₂(Fe,Co,Zr)₁₄B- α -Fe and Nd(Fe,Mo)₁₂N_x- α -Fe powders. *J. Alloys Com.* **230**(1), L1–L3 (1995). [https://doi.org/10.1016/0925-8388\(95\)01979-0](https://doi.org/10.1016/0925-8388(95)01979-0)
39. Jurczyk, M., Jakubowicz, J.: Nanocomposite Nd₂(Fe,Co,Cr)₁₄B/ α -Fe materials. *J. Magnet. Magn. Mat.* **185**(1), 66–70 (1998). [https://doi.org/10.1016/S0304-8853\(97\)01160-8](https://doi.org/10.1016/S0304-8853(97)01160-8)
40. Jakubowicz, J., Jurczyk, M., Handstein, A., Hinz, D., Gutfleisch, O., Müller, K.H.: Temperature dependence of magnetic properties for nanocomposite Nd₂(Fe,Co,M)₁₄B/ α -Fe magnets. *J. Magnet. Magn. Mat.* **208**(3), 163–168 (2000). [https://doi.org/10.1016/S0304-8853\(99\)00587-9](https://doi.org/10.1016/S0304-8853(99)00587-9)

Publisher's Note Springer Nature remains neutral with regard to jurisdictional claims in published maps and institutional affiliations.